



Preparation and Characterization of Nano ZnFe₂O₄ Supported on Copper Slag and its Effects on the Degradation of *p*-Xylene Aqueous Solution

Hossein Malekhosseini¹, Morteza Khosravi¹, Kazem Mahanpoor^{2*}, Fereshteh Motiee¹

¹Department of Chemistry, Tehran North Branch, Islamic Azad University, Tehran, Iran

²Department of Chemistry, Arak Branch, Islamic Azad University, Arak, Iran

(Received 23 May 2019; Final revised received 15 Aug. 2019)

Abstract

One of the problems in removing pollutants from water by photocatalytic methods is the separation of the catalyst from the solution. In this study, the catalyst stabilization method was used to solve this problem. Nano ZnFe₂O₄ supported on Copper Slag (CS) produced in this research is an environment-friendly, simple and cost-effective catalyst. ZnFe₂O₄ was prepared for co-precipitation methods and supported on CS by the thermal process. Its characterization was done by scanning electron microscopy (SEM) images, energy-dispersive X-ray spectroscopy (EDX), BET surface area and X-Ray diffraction patterns (XRD). The degradation of *p*-Xylene as a pollutant in water was performed by the UV + H₂O₂ process using ZnFe₂O₄/CS as a photocatalyst. Circulate Packed Bed Reactor (CPBR) was used. For photocatalytic degradation of the *p*-Xylene, full factorial experimental design with three factors containing pH, the initial concentration of *p*-Xylene and H₂O₂ in three levels was used. The best conditions were determined as pH= 9, the concentration of *p*-Xylene= 70 ppm and concentration of H₂O₂= 20 ppm. Degradation efficiency in the best condition was 95.40 %. This new catalyst can also be used in processes for organic pollutant degradation.

Keywords: Photocatalyst, Full factorial, Photodegradation, Optimization.

*Corresponding author: Kazem Mahanpoor, Department of Chemistry, Arak Branch, Islamic Azad University, Arak, Iran, E-mail: k-mahanpoor@iau-arak.ac.ir, Tel: +988634132451-9, fax: +988634132273.

Introduction

Benzene (B), Toluene (T), Ethylbenzene (E) and *p*-Xylene (X) jointly known in short as BTEX are hazardous substances that are used as a solvent in many chemical industries. Since BTEX are carcinogenic and toxic substances, excessive amounts of them in a water environment may have a negative effect on water quality and thus jeopardize public health [1]. They are commonly found in the various industrial process and effluents. It is so obvious that the efficient wastewater treatment of BTEX is necessary. *p*-Xylene is an important raw material for chemical industry applications such as in the synthesis of different polymers. Specifically, it is a component in manufacturing Terephthalic acid for the production of polyesters like polyethylene terephthalate. It may also directly produce poly (*p*-Xylene).

Many conventional treatments process, e.g. biological methods and physicochemical methods (catalytic oxidation-reduction and membrane separation) are used for the degradation of the *p*-Xylene aqueous solution. Among various methods of elimination of *p*-Xylene, the use of photocatalysis is one of the most appealing methods. The photocatalytic degradation of aqueous phase volatile organic compounds such as *p*-Xylene by semiconductors is a relatively slow process. There are many limitations (e.g. safety matters and the use of powder materials) for large-scale applications [2, 3]. There are a few examples of AOP application for the degradation of BTEX in aqueous solutions using UV/H₂O₂, ozonation and Fenton systems [4-10]. Among these AOPs, the UV/H₂O₂ process is five times faster in degrading aromatic compounds than others [11,12]. Various catalysts including doped TiO₂ (N-TiO₂ and Fe-TiO₂), TiO₂ and Bentonite-TiO₂ in the photocatalytic removal process of *p*-Xylene aqueous solution were studied under various conditions. The results of this research show that Bentonite-TiO₂ is the best photocatalyst for the *p*-Xylene degradation process [13].

Researchers reported the use of the ozone/UV process in removing BTEX, MTBE, tert-Butyl alcohol and petroleum hydrocarbons from gasoline present in contaminated groundwater samples. After treatment under before established experimental conditions, removal indices higher than 99% of pollutants initially present in all contaminated water samples were obtained [14]. Powder photocatalysts cannot be easily recycled and may cause secondary pollution [3]. Thus, a need arises for preparing photocatalysts stabilized on the support materials with suitable surface areas. ZnFe₂O₄, similar to TiO₂, is one of the most used photocatalysts because of its relatively long lifetime of the electron-hole pairs and chemical stability [15-17]. UV irradiation over ZnFe₂O₄ can efficiently generate electron-hole pairs that induce strong oxidizing agents similar to hydroxide (OH°) and peroxide ($O_2^{\circ-}$) radicals by interacting with H₂O and dissolved O₂ in aqueous solution.

These radicals can decompose VOCs into non-toxic molecules such as CO₂ and H₂O. The main problem is the separation of the catalyst from the solution [16-17].

One way to eliminate this problem is to fix the catalyst on a suitable base. As Copper Slag (CS) is cheaper and stable, it was chosen as the base of the ZnFe₂O₄ for the increasing catalyst surface. Mechanical and thermal properties of CS are suitable for supporting the catalyst. Nano ZnFe₂O₄ supported on CS a new environment-friendly catalyst was prepared in this study. This catalyst was characterized by SEM images, X-Rays diffraction patterns and BET. UV + H₂O₂ process and ZnFe₂O₄/CS, as a photocatalyst were used for the degradation of the *p*-Xylene.

The full factorial method is a set of statistical techniques in applied mathematics for modeling experimental results. This procedure can be used for studying the effect of several factors (with different levels) and their influences on each other. For photocatalytic degradation of the *p*-Xylene process, three factors and three levels of full factorial experimental design were used [16-22]. All variables are assumed to be measured. The full factorial experimental design can be expressed as an Equation (1):

$$Y = f(x_1, x_2, x_3 \dots x_i) \quad (1)$$

This research aims at optimizing the response variable (Y). The assumption is that the independent variables x_i is continuous, and trial and error control are negligible. The research objective is to find a good approximation for the functional link between independent variables and the equation superior. This factorial design resulted in 12 tests of possible combinations of x_1 , x_2 , and x_3 . Photocatalytic degradation, efficiency (Y) was measured for each test. The first-order model with all possible interactions was chosen to fit the experimental Equation 2:

$$Y = B_0 + B_1x_1 + B_2x_2 + B_3x_3 + B_{12}x_1x_2 + B_{13}x_1x_3 + B_{23}x_2x_3 + B_{123}x_1x_2x_3 \quad (2)$$

Now research, the photocatalytic degradation of the *p*-Xylene aqueous solution was studied in Circulating Packed Bed Reactor (CPBR) using ZnFe₂O₄/CS as a new supported photocatalyst. The experimental work is carried out using full factorial design to examine the main effects and the interactions between pH, initial concentration of *p*-Xylene H₂O₂. Optimization of the process parameters affecting the photocatalytic process was made by a three-level and three factors full factorial experimental design by Minitab 17.2 software [18-22].

Experimental

Materials

p-Xylene, Zinc and Iron nitrate salt and other materials used for the study were produced by Merck Company, Germany. CS purchased from an Iranian company, Messbareh.

The preparation of ZnFe₂O₄/CS

50 ml Zinc nitrate (0.25 M) solutions (prepared from Zn(NO₃)₂·6H₂O) was added to the 50 ml (0.5 M) Ferric nitrate solutions (prepared from Fe(NO₃)₃·9H₂O). 100 ml, urea solutions (2M) were added to this solution refluxed for 12 hours. The precipitates were isolated and dried at 110 °C. The precipitate was heated in a furnace at 550 °C for 4 hours. CS was then mixed with ZnFe₂O₄ powder and put into the furnace at 550 °C for 6 hours.

The characterization of ZnFe₂O₄/CS

The shape, size and surface morphology of the synthesized ZnFe₂O₄/CS were examined by the images of a Philips XL-30 SEM. The X-Ray Diffraction (XRD) analysis of the samples was done by a DX27-mini diffractometer. BET surface area of materials was determined by the N₂ adsorption-desorption method of 77 K, measured by BELSORP-mini II instruments. The samples were degassed under a vacuum at 473 K for 12 hours before the BET measurement.

The experimental procedure

Schematic view of the apparatus is in Figure 1. CPBR with a volume of 1 liter (the effective volume of 0.2 liters) was used. A UV lamp with the power of 15 W, Philips, was placed directly in the reactor. The UV lamp was surrounded by the catalyst. The CPBR was surrounded by 70 grams of catalyst ZnFe₂O₄ / CS. For photocatalytic degradation experiments, Sodium hydroxide and Sulfuric acid, diluted solutions were used to adjust the pH of solutions. Furthermore, a Metrohm pH meter model 827 was used for measuring pH amounts. The different volume levels of Hydrogen peroxide were added to the *p*-Xylene solution. The solutions were transferred to the feed tank and sent into the reactor by a water pump. After half an hour of rotation of the solution on the reactor, the UV lamp was turned on. Every 10 minutes, some samples were taken and their CODs were measured by Standard Method (5220). All Ultraviolet/Visible (UV/Vis) absorption spectra for determining COD was obtained by an Agilent 8453 spectrophotometers. The percentage removal of *p*-Xylene was calculated by using the following equation 3:

$$\% R = \frac{COD_0 - COD}{COD_0} \times 100 \quad (3)$$

Where R is removal efficiency (%), COD_0 is the initial chemical oxygen demand value of p -Xylene solution and COD is the chemical oxygen demand value of p -Xylene solution after photo-irradiation.

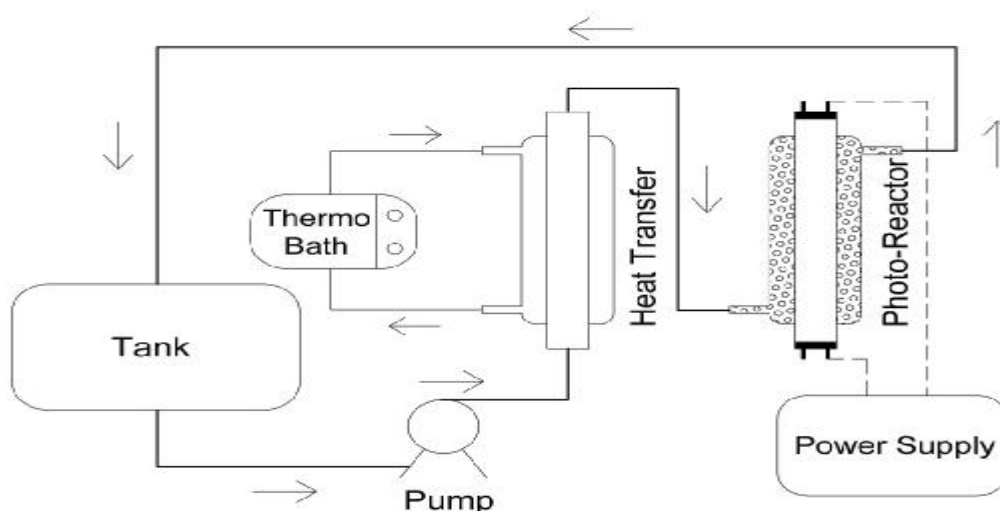


Figure 1. The schematic view of the experimental apparatus.

Full factorial experimental design

By the Full Factorial experimental design method, several experiments were conducted and factors influencing the photocatalytic degradation (pH, the initial concentration of p -Xylene ($C_{p\text{-Xylene}}$) and concentration of Hydrogen peroxide ($C_{H_2O_2}$) were studied. The experimental range and levels of variables are in Table 1. The low and high levels were selected for factors for some initial experiments. At three levels, pH 5, 7 and 9, the initial concentration of p -Xylene from 70, 100 and 130 ppm and initial H_2O_2 concentration from 20, 30 and 40 ppm. In Table 2, 12 experiments related to this factorial design and their experimental conditions have been listed. The removal efficiency of p -Xylene was a dependent response. To do DOEs Minitab, 17 version 17.2 statistical software was used. Analysis of variance (ANOVA) was also used to interpret the results.

Table 1. The experimental range and levels of variables

Variables	Range and levels		
	-1	0	+1
pH	5	7	9
Initial Con. of p -Xylene (ppm)	70	100	130
H_2O_2 Concentration (ppm)	20	30	40

Table 2. Experimental conditions for the photocatalytic process

Exp. No	pH	Initial Con. of p-Xylene (ppm)	H ₂ O ₂ Con. (ppm)
1	5	130	20
2	9	70	20
3	9	130	20
4	5	130	40
5	7	100	30
6	9	130	40
7	7	100	30
8	5	70	40
9	5	70	20
10	7	100	30
11	9	70	40
12	7	100	30

Results and discussion

Catalyst identification

The catalyst was identified by XRD and SEM devices. The corresponding powder X-ray diffraction (XRD) pattern provides further crystallinity about the resultant ZnFe₂O₄. The observed peak positions (as shown in Figure 2) are consistent with the characteristic peaks reported for ZnFe₂O₄ [23]. Fayalite (2FeO.SiO₂) with specified peaks being $2\theta = 52$ was the main crystalline phases in CS. The specific peaks of Magnetite (Fe₃O₄), Hedenbergite Ca (Fe, Mg) (SiO₃)₂, Hematite and Magnetite range from $2\theta = 28$ to $2\theta = 31$ [24,25]. Moreover, the mean sizes of the as-synthesized nanoparticles were calculated from the peak broadening in the XRD pattern by using the Debye-Scherrer formula. [26] The average sizes of ZnFe₂O₄ were 65 nanometers.

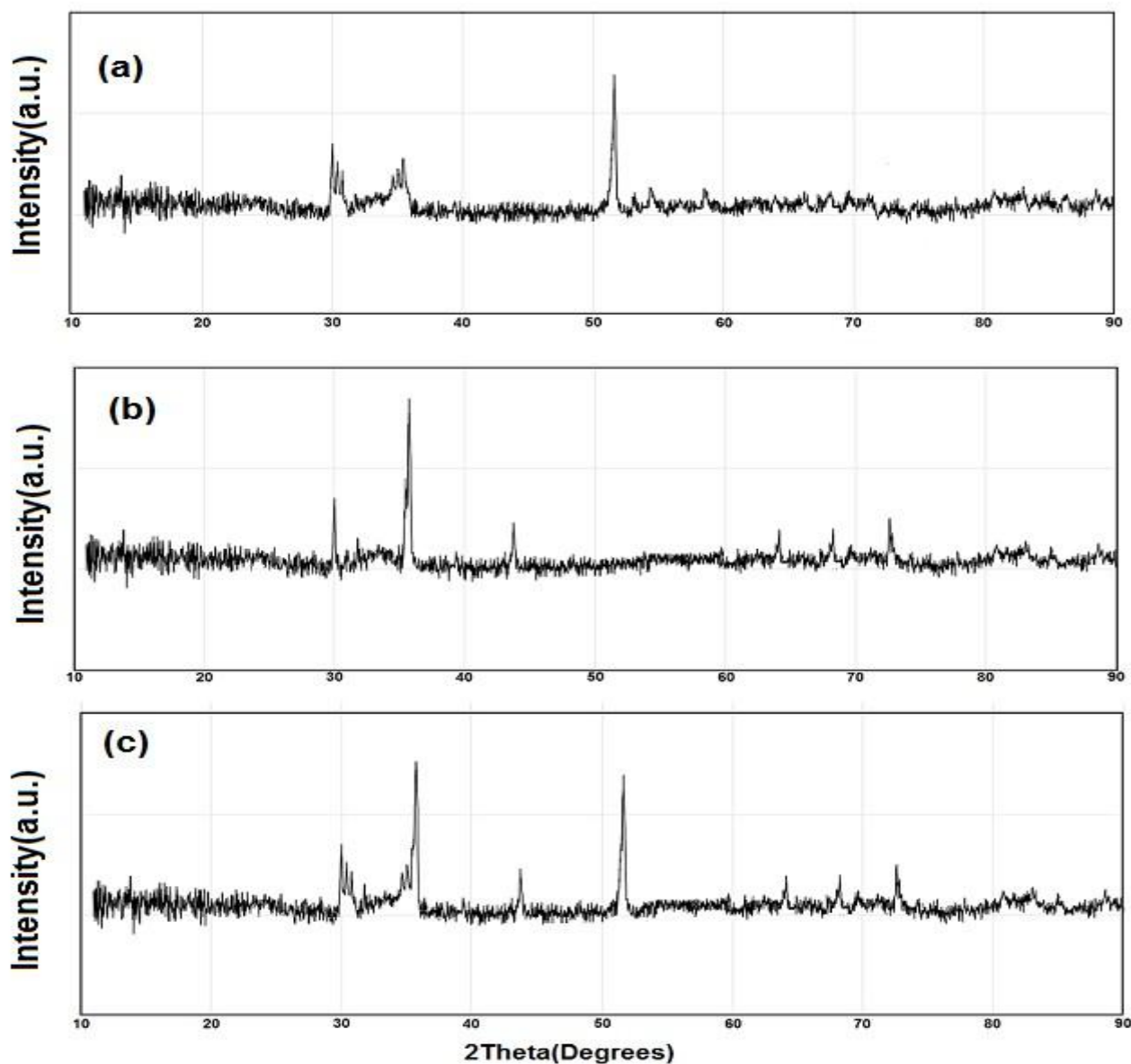


Figure 2. The XRD patterns of photocatalyst for a) CS b) ZnFe₂O₄, and c) ZnFe₂O₄ / CS.

The surface morphology and the approximate particle sizes of the ZnFe₂O₄ were characterized by SEM. The results (Figure 3) show that the surfaces of particles are smooth, homogeneous and very similar to Nano-spherical particles. The sizes of particles are varied but have a similar shape. As shown in Figure.3, all surfaces of CS are covered with ZnFe₂O₄nanoparticle. EDX analysis of product also proved that substances which have been established on the surface consist only of ZnFe₂O₄nanoparticle.

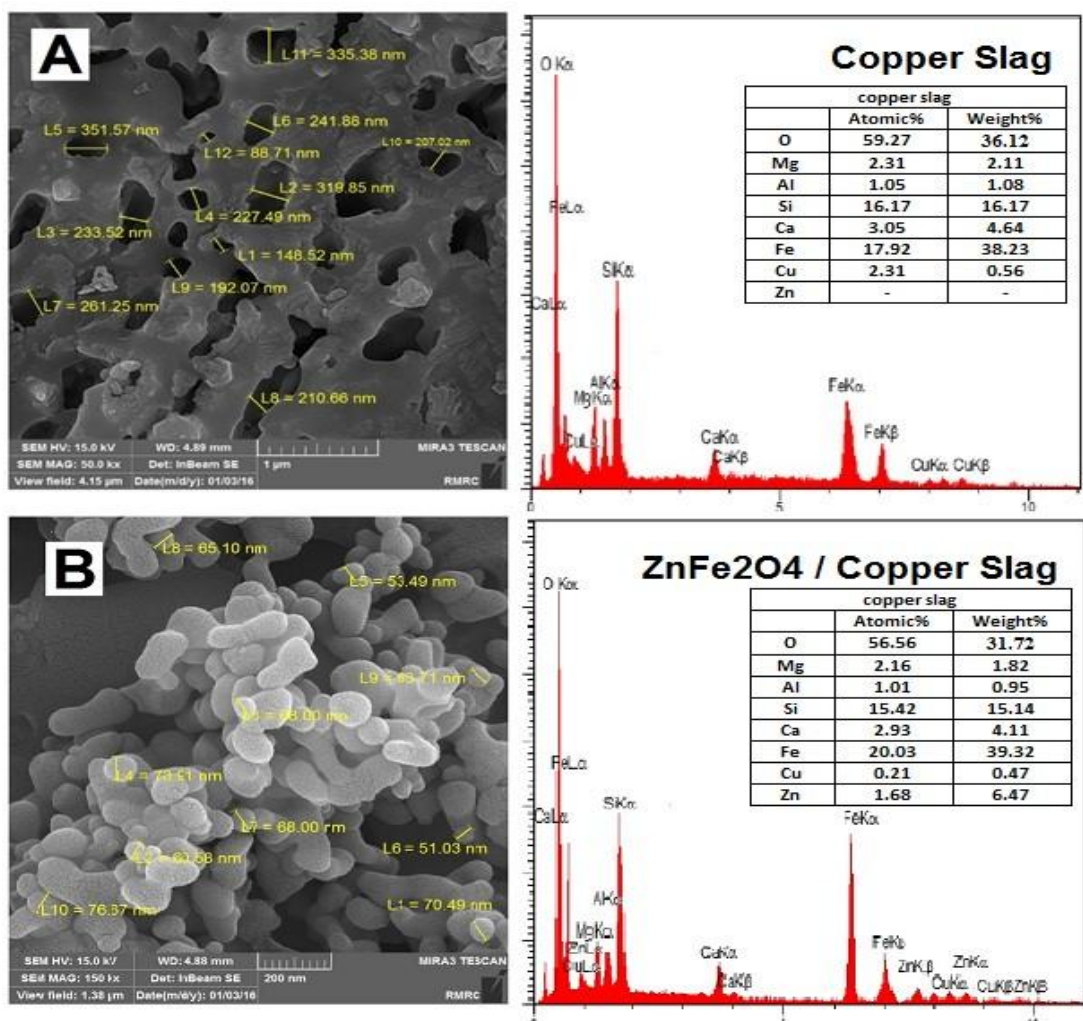


Figure 3. SEM images and their EDX analysis of A) CS and B) ZnFe₂O₄ / CS.

Low-temperature (77 K) nitrogen adsorption-desorption isotherms were used for pore structure analysis of porous materials. The Brunauer–Emmett–Teller (BET) method was used for the determination of the surface area of the new materials. Figure 4 shows the adsorption-desorption isotherms and BET surface area for the CS and ZnFe₂O₄/CS. The adsorption isotherms of the CS samples are of type IV. The hysteresis loops of the samples are H₂ type classification [27]. It indicates that the structure is mainly mesoporous, with pores being narrow mouths (ink-bottle pores). Bottleneck (cylindrical pore geometry) pores and spherical particles are the same for ZnFe₂O₄ and ZnFe₂O₄/CS. The BET surface area of CS and ZnFe₂O₄/CS were determined 3.21 and 16.25 (m²/g), respectively. It seems that supporting nanoparticle ZnFe₂O₄ on the CS has increased the BET surface area of the catalyst.

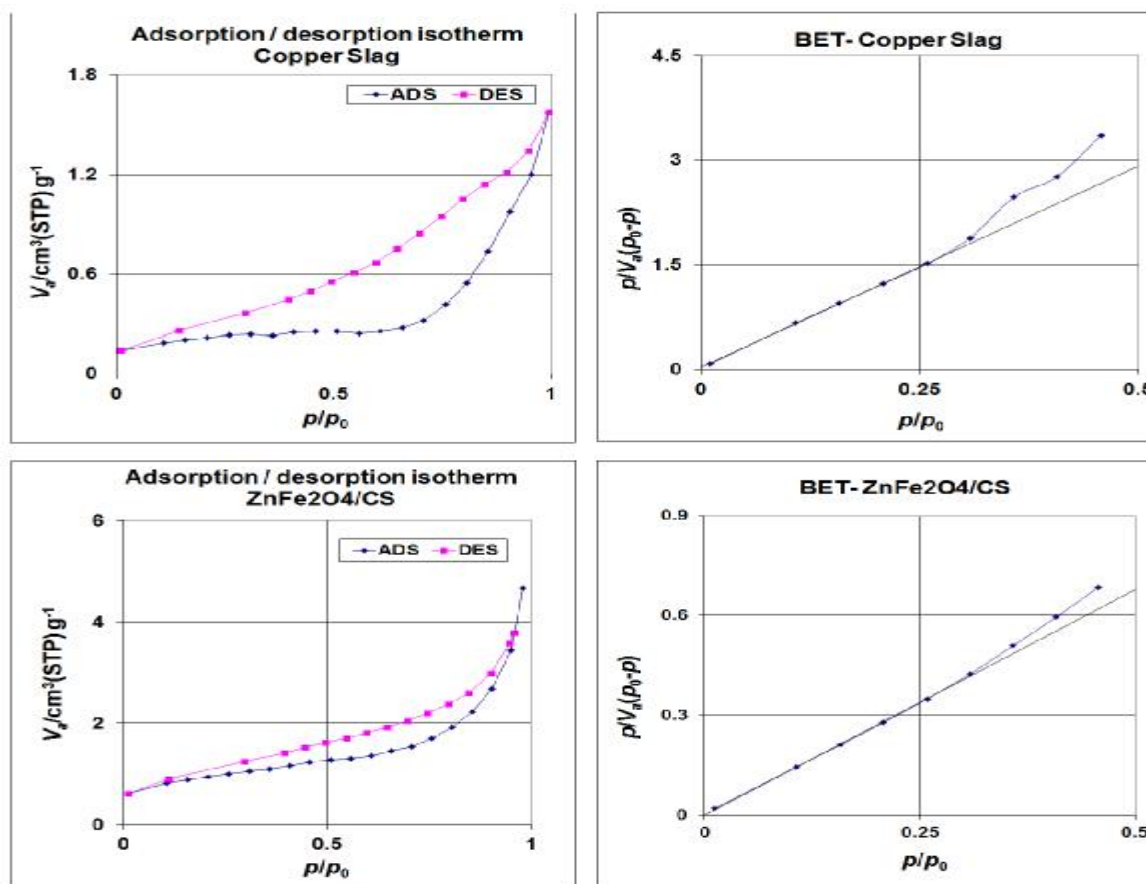


Figure 4. Adsorption-desorption isotherms and BET surface area for the CS and ZnFe₂O₄/CS.

The statistical analysis and optimum conditions

The test of ANOVA was used for analyzing the data. The quality of the fit polynomial model was expressed with the coefficient of determination (R^2). The statistical significance of the model was checked by Fisher's test (F-test). Model terms were evaluated by the P-value. In Table 3, the estimated effects and coefficients for removal (%) have been listed. In this table, the standard deviation (S), correlation coefficient, pried R-squared and adjusted R-squared amounts were also reported. The square of the correlation coefficient for each response was computed as R^2 . The accuracy and variability of the model can be evaluated by R^2 .

The best model for predicting the response (removal (%)) is that the value of R^2 close to 1. R^2 values was reported as 0.9998 in this paper. The predicting R-squared of 0.9941 is in reasonable agreement with the adjusted R-squared of 99.96, confirming good predictability of the model. According to Table 3 and the significant variable effects on the response, the magnitudes of the initial concentration of *p*-Xylene and H₂O₂ as well as pH are equal to -18.376, -1.2275 and 5.782, respectively. Thus, the significant reaction parameters from the most to the least significant were: initial concentration of *p*-Xylene > pH > initial concentration of H₂O₂. It should be noted that despite

the other three variables, the variable of the initial concentration of *p*-Xylene has a negative effect on the response (-18.376). This means that increasing the initial concentration of *p*-Xylene leads to decreasing removal (%) and vice versa. In this way, the effects of the variables and the interaction were reported in Table 3. The results show that the interaction of variables, i.e. the initial concentration of *p*-Xylene and the H₂O₂ concentration, has positive effects (5.782). The interaction of the initial concentration of H₂O₂ with pH has negative effects on the removal (%) value (-12.918). In Table 3, the coefficients of each term have been reported. They are the same term coefficients in response function given in Equation (3).

It should be noted that P values have been assessed considering $\alpha=0.05$. Table 4 depicts the results of ANOVA. The effects on the response were increased by increasing the value of the F and decreasing P. For main effects (with 3 degrees of freedom) – the *p*-Xylene initial concentration, pH and H₂O₂ concentration- F and P values have been obtained as 4947.92 and <0.0001, respectively. Furthermore, these values were 6694.21 and <0.0001 for 2-way interactions (with 2 freedom degrees of freedom), respectively. In Table 5, complementary results used for drawing residual plots have been listed. Residual values were calculated by subtracting experimental removal (%) values from fitted values.

Table 3. Estimated effects and coefficients for the removal(%).

Terms	Effect	Coef.	SE Coef.	T-value	P-value	VIF
Constants	-	71.969	0.0791	910.20	0.000	1.00
pH	-1.2275	-0.6137	0.0968	-6.34	0.001	1.00
Initial Con. of p-Xylene	-18.376	-9.0188	0.0968	-93.13	0.000	1.00
H₂O₂	5.782	2.8912	0.0968	29.86	0.000	1.00
Initial Con. of p-Xylene × pH	0.8425	0.4212	0.0968	4.35	0.007	1.00
H₂O₂ × pH	-12.918	-6.4588	0.0968	-66.70	0.000	1.00
Initial Con. of p-Xylene × H₂O₂	24.203	12.101	0.0968	124.96	0.000	1.00

R²=99.98, Pred R²=99.41, Adj R²=99.96

Table 4. ANOVA results.

Sources	Degrees of freedom	Adj SS	Adj MS	F- value	P-value
model	6	2227.26	371.21	4947.92	0.000
Linear	3	720.59	240.20	3201.63	0.000
pH	1	3.01	3.01	40.17	0.001
Initial Con. of p-Xylene	1	650.70	650.70	8673.34	0.000
H ₂ O ₂	1	66.87	66.87	891.38	0.000
2-Way Interactions	3	1506.67	502.22	6694.21	0.000
Initial Con. of p-Xylene × pH	1	1.42	1.42	18.92	0.007
pH × H ₂ O ₂	1	333.72	333.72	4448.26	0.000
Initial Con. of p-Xylene × H ₂ O ₂	1	1171.52	1171.52	15615.44	0.000
Errors	5	0.38	0.08		
Lack-of-fit	2	0.37	0.18	67.97	0.003
Pure Errors	3	0.01	0.00		
Total	11	2227.63			

Table 5. Residual values.

Exp. No.	Removal (%)	Fit	Residual (Removal(%)–Fit)
1	41.47	41.6917	-0.2217
2	95.40	95.6217	-0.2217
3	54.43	54.2242	0.2058
4	84.80	84.5942	0.2058
5	72.05	71.9692	0.0808
6	71.07	71.2917	-0.2217
7	71.96	71.9692	0.0092
8	79.05	79.2717	-0.2217
9	84.98	84.7742	0.2058
10	72.00	71.9692	0.0308
11	64.49	64.2842	0.2058
12	71.93	71.9642	-0.0342

Figure 5 which is a Pareto chart of standardized effects can be used to compare variables effects on the response. The results revealed that the effect of the initial concentration of *p*-Xylene on the removal (%) is greater than the other variables effects, but its effect is negative, for example increasing the initial concentration of *p*-Xylene leads to decreasing the removal (%), and vice versa. A mathematical model representing *p*-Xylene photocatalytic degradation in the range of the study can be expressed by Equation (3):

$$R(\%) = 71.9692 - 0.6137 \times (\text{pH}) - 9.0188 \times (\text{p-Xylene}) + 2.8912 \times (\text{H}_2\text{O}_2) + 0.4212 \times (\text{pH} \times \text{p-Xylene}) - 6.4588 \times (\text{pH} \times \text{H}_2\text{O}_2) + 12.1013 \times (\text{p-Xylene} \times \text{H}_2\text{O}_2) \quad (3)$$

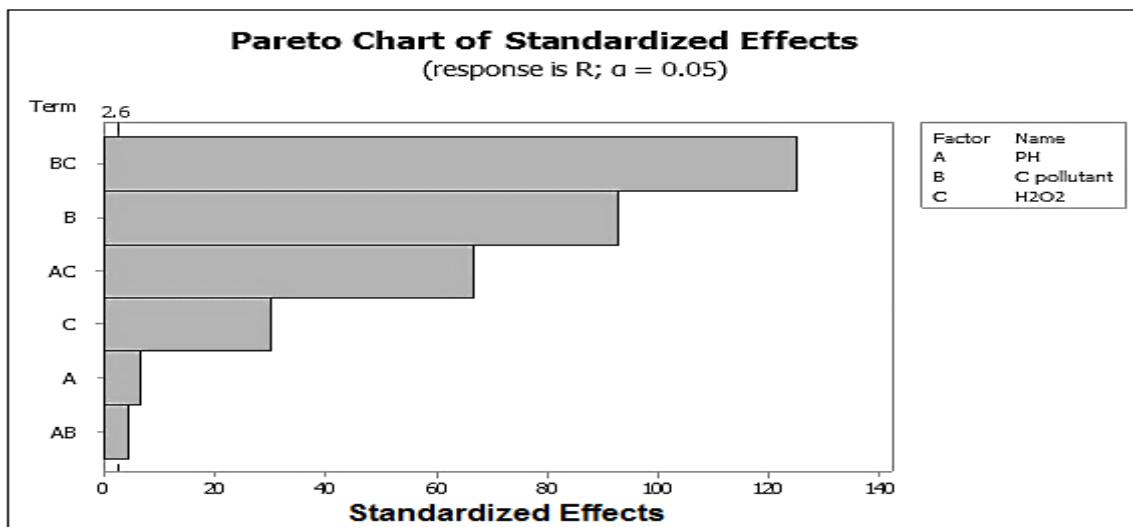


Figure 5. Pareto charts of standardized effects.

To determine the reusability of the catalyst, the experiments were repeated to determine the optimal conditions. Results are respectively as follows: $R_1 = 95.40$, $R_2 = 95.27$, $R_3 = 95.02$, $R_4 = 94.98$, $R_5 = 94.96$. These results show that the reusability of the catalyst is acceptable.

Conclusion

The $\text{ZnFe}_2\text{O}_4/\text{CS}$ synthesis method is easy and cost-effective. Using this catalyst, the problem of separating the catalyst from the aqueous solution is eliminated in the photocatalytic process. Since CS is a solid waste, the use of CS as a catalyst base reduces considerably environmental contamination. The results of the study show that it is advisable to use CS as the basis for a new stable photocatalyst. The statistical analysis results obtained from the full factorial experiment design indicated that the model used in this study is much reliable and valid. The interactions of the variables are also very important and due to the significant effects of these interactions on the removal(%), they should be optimized. The full factorial experimental design is a suitable method for optimizing and modeling similar processes.

Acknowledgment

The authors are thankful to Islamic Azad University, North Tehran Branch and Arak Branch for their laboratory support.

References

- [1] Y.W. Fan, Q.X. Zhou, *Chin. J. Ecol.*, 27, 632 (2008).
- [2] T. Soltani, B.K. Lee, *J. Hazard. Mater.*, 316, 122 (2016).
- [3] F. Moulis, J. Krysa, *Catal. Today.*, 209, 153 (2013).
- [4] R. Andreozzi, V. Caprio, A. Insola, R. Marotta, R. Sanchirico, *Water Res.*, 34, 620(2000).
- [5] P. Stepnowski, E.M. Siedlecka, P. Behrend, B. Jastorff, *Water Res.*, 36, 2167 (2002).
- [6] J. Saien, H.Nejati, 2007. *J. Hazard. Mater.*, 148, 491 (2007).
- [7] G. Hu, J. Li, G. Zeng, *J. Hazard. Mater.*, 261, 470 (2013).
- [8] M. Bahmani, V. Bitarafhaghighi, K. Badr, P. Keshavarz, D. Mowla, *Desalin. Water Treat.*, 52, 3054 (2014).
- [9] H. Huang, H. Huang, Y. Zhan, G. Liu, X. Wang, H. Lu, L. Xiao, Q. Feng, D.Y.C. Leung, *Appl. Catal. B.*, 186, 62 (2016).
- [10] Y. Xue, S. Lu, X. Fu, V.K. Sharma, I. Mendoza-Sanchez, Z. Qiu, Q. Sui, 2018. *Chem. Eng. J.*, 331, 255 (2018).
- [11] M. Barrera, M. Mehrvar, K. Gilbride, L. McCarthy, A. Laursen, V. Bostan, R. Pushchak, *Chem. Eng. Res. Des.*, 90, 1335(2012).
- [12] C.F. Bustillo-Lecompte, M. Knight, M. Mehrvar, *Can. J. Chem. Eng.*, 93, 798 (2015).
- [13] C. Liu, J. F. Chen, R.C. Chen, *Int. J. Nanosci.*, 14, 1460022 (2015).
- [14] C. F.B.Lecompte, D. Kakar, M. Mehrvar, *J. Cleaner. Prod.*, 186, 609 (2018).
- [15] E. Casbeer, V.K. Sharma, X.Z. Li, *Sep. Purif. Technol.*, 87, 1 (2012).
- [16] M. Chandrika, A.V. Ravindra, C. Rajesh, S.D. Ramarao, S. Ju, *Mater. Chem. Phys.*, 230, 107 (2019).
- [17] M. Nikazar, K. Gholivand, K. Mahanpoor, *Desalination.*, 219, 293 (2008).
- [18] V.A. Sakkas, M.A. Islam, C. Stalikas, T.A. Albanis, *J. Hazard. Mater.*, 175, 33 (2010).
- [19] M. Saghi, K. Mahanpoor, *Int. J. Ind. Chem.*, 8, 297 (2017).
- [20] A. Shokri, *Int. J. Ind. Chem.*, 56, 765 (2018).
- [21] J.Fernández, J. Kiwi, C.Lizama, J. Freer, J. Baeza, H.D. Mansilla, *J. Photochem. Photobiol. A.*, 151, 213 (2002).
- [22] M.C. Yeber, C. Soto, R. Riveros, J. Navarrete, G. Vidal, *Chem. Eng. J.*, 152, 14 (2009).
- [23] Z.H. Zhou, J.M. Xue, H.S.O. Chan, J. Wang, *Mater. Chem. Phys.*, 75, 181 (2002).
- [24] V.K. Marghussian, A. Maghsoodipoor, *Ceram. Int.*, 25, 617 (1999).
- [25] R.C. Sripriya, M. Mahendiran, J. Madahavan, M.V.A. Raj, *Mater. Today: Proc.*, 8, 310 (2019).
- [26] S. Sarkar, R. Das, *Indian J. Pure Appl. Phys.*, 56, 765 (2018).

[27] K.S.W. Sing, D.H. Everett, R.A.W. Haul, L. Moscou, R.A. Pierotti, J. Rouquerol, T. Siemieniwska, *Pure Appl. Chem.*, 57, 603 (1985).